

# Spatial Localization and Quantitation of Androgens in Mouse Testis by Mass Spectrometry Imaging

Diego F. Cobice,<sup>†,¶,∇</sup> Dawn E. W. Livingstone,<sup>†,‡,¶</sup> C. Logan Mackay,<sup>§</sup> Richard J. A. Goodwin,<sup>||</sup> Lee B. Smith,<sup>⊥</sup> Brian R. Walker,<sup>†</sup> and Ruth Andrew<sup>\*,†</sup>

<sup>†</sup>University/British Heart Foundation Centre for Cardiovascular Science, Queen's Medical Research Institute, University of Edinburgh, 47 Little France Crescent, Edinburgh, EH16 4TJ, United Kingdom

<sup>‡</sup>Centre for Integrative Physiology, University of Edinburgh, Hugh Robson Building, 15 George Square, Edinburgh EH8 9XD, United Kingdom

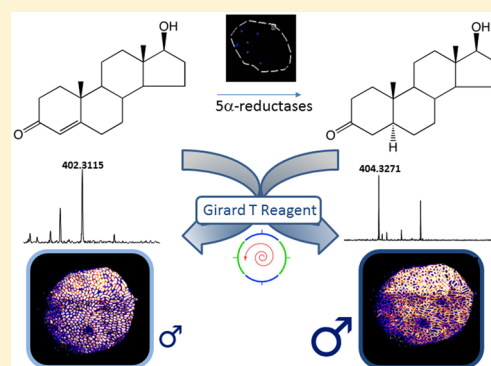
<sup>§</sup>SIRCAMS, School of Chemistry, University of Edinburgh, Joseph Black Building, The King's Buildings, West Mains Road, Edinburgh, EH9 3JJ, United Kingdom

<sup>||</sup>AstraZeneca R&D, Cambridge, CB4 0WG, United Kingdom

<sup>⊥</sup>MRC Centre for Reproductive Health; Queen's Medical Research Institute, University of Edinburgh, 47 Little France Crescent, Edinburgh, EH16 4TJ, United Kingdom

## S Supporting Information

**ABSTRACT:** Androgens are essential for male development and reproductive function. They are transported to their site of action as blood-borne endocrine hormones but can also be produced within tissues to act in intracrine and paracrine fashions. Because of this, circulating concentrations may not accurately reflect the androgenic influence within specific tissue microenvironments. Mass spectrometry imaging permits regional analysis of small molecular species directly from tissue surfaces. However, due to poor ionization and localized ion suppression, steroid hormones are difficult to detect. Here, derivatization with Girard T reagent was used to charge-tag testosterone and  $5\alpha$ -dihydrotestosterone allowing direct detection of these steroids in mouse testes, in both basal and maximally stimulated states, and in rat prostate. Limits of detection were  $\sim 0.1$  pg for testosterone. Exemplary detection of endogenous steroids was achieved by matrix-assisted laser desorption ionization and either Fourier transform ion cyclotron resonance detection (at  $150 \mu\text{m}$  spatial resolution) or quadrupole-time-of-flight detection (at  $50 \mu\text{m}$  spatial resolution). Structural confirmation was achieved by collision induced fragmentation following liquid extraction surface analysis and electrospray ionization. This application broadens the scope for derivatization strategies on tissue surfaces to elucidate local endocrine signaling in health and disease.



Androgens are essential regulators of male development and adult reproductive function, primarily synthesized within the testis. During embryonic development, testicular fetal Leydig and Sertoli cells work in concert to produce testosterone.<sup>1,2</sup> This is converted into the most active androgen,  $5\alpha$ -dihydrotestosterone (DHT), by  $5\alpha$ -reductases in peripheral tissues to promote masculinization and normal size of target organs.<sup>3–5</sup> In postnatal life, a second population of (adult) Leydig cells develops superseding the fetal population; these Leydig cells complete all steps of steroidogenesis to produce and secrete testosterone throughout adulthood.<sup>6</sup> Additional androgens, androstenedione (A4) and dehydroepiandrosterone (DHEA), are synthesized in the adrenal glands in many species but not rats or mice.<sup>7,8</sup> Androgens have pleiotropic functions in the testis, e.g., completion of meiosis, differentiation of spermatids, initiation of spermatogenesis at puberty, and maintenance of this process in the adult.<sup>9</sup> Dysregulation of these processes may lead to

testicular dysfunction and infertility. In contrast, increased androgen signaling plays a role in pathologies, including benign prostatic hyperplasia (BPH) and prostate cancer.<sup>10,11</sup>

Liquid chromatography-tandem mass spectrometry (LC-MS/MS) is the method of choice for quantifying circulating androgens, but little information is available relating circulating to tissue levels due to analytical limitations. While androgens may be quantified in extracts of biopsies,<sup>7,12</sup> this does not spatially align steroid levels with subregions, e.g., cell types or tumors. Retaining spatial distribution of androgens can be crucial, for example, in androgen-sensitive prostate tumors, where the cellular activities of  $5\alpha$ -reductases are critical to the local exposure to DHT. Mass spectrometry imaging (MSI) is gaining

Received: June 9, 2016

Accepted: September 27, 2016

Published: September 27, 2016

traction as a bioanalytical tool to map spatial distribution of small molecules in tissues and identify, localize, and relatively quantitate compounds in complex biological matrices.<sup>13</sup> Many small molecule applications of MSI pertain to drug discovery, but we recently validated a MSI approach for assessing the spatial distribution of glucocorticoids in murine brain.<sup>14</sup> On-tissue chemical derivatization (OTCD) using Girard T (GirT) reagent overcame poor target ionization efficiency and ion suppression, and the increased  $m/z$  helped avoid interference of matrix-related background in the lower mass range. GirT reagent reacts with ketones<sup>15</sup> and enhances sensitivity in the measurement of lipophilic steroids within tissue matrix, but the approach requires skillful and flexible manual application. Glucocorticoids are pregnene steroids, with several ketones, the most reactive being at C3 in the A-ring, conjugated with a C4–5 double bond (Nomenclature of steroids, Figure S-1). The endogenous androgens, testosterone and androstenedione, contain a similar ketonic function and may also be derivatized using hydrazine-based reagents<sup>15</sup> (Derivatization Reactions, Figure S-1). A recent report suggests derivatization with GirT is useful for MSI of testosterone in tissue.<sup>16</sup> However, within tissue, testosterone levels must be interpreted in conjunction with those of the more potent DHT. The A-ring of DHT is reduced, and the ketone is less activated (not allylic to the  $\Delta 4-5$  double bond) and thus less amenable to derivatization.

Here, we describe how OTCD with MSI can spatially localize testosterone and DHT in rodent reproductive tissues. Translational challenges and methodological improvements to reduce diffusion and increase robustness by inclusion of automated spraying technology are reported for the first time.

## ■ EXPERIMENTAL SECTION

**Sources of Chemicals.** Internal standard [<sup>2</sup>H]<sub>8</sub>-cortisone-2,2,4,6,6,7,21,21 (*d*<sub>8</sub>-CORT) was from Cambridge Isotopes, MA, USA; unlabeled steroids were obtained from Steraloids Inc., PA, USA. Solvents were glass-distilled HPLC grade (Fisher Scientific, Loughborough, UK). Other chemicals were from Sigma-Aldrich (Dorset, UK) unless stated. Room temperature (RT) was 18–21 °C.

**Animals and Biomatrix Collection.** C57BL/6 mice (Harlan Olac Ltd., Bicester, UK) were studied under UK Home Office license. To stimulate androgen biosynthesis, human chorionic gonadotrophin (hCG, 20 IU, Organon, The Netherlands) or vehicle (saline) was administered by subcutaneous injection to male mice (aged 8–10 weeks;  $n = 3/\text{group}$ ) and testes and blood were collected following cull by CO<sub>2</sub> 16 h later. Plasma (EDTA) was prepared by centrifugation (10 000g, 5 min, 4 °C). Tissues were snap frozen in liquid nitrogen and stored (–80 °C). Concentrations of testosterone in plasma were quantified by LC-MS/MS.<sup>17</sup> Prostates were similarly collected from male Sprague–Dawley rats (Harlan Olac Ltd.).

**Reaction Efficiency: LC-MS/MS Analysis of Nonderivatized and Derivatized Steroids.** Steroid (1  $\mu\text{g}/10 \mu\text{L}$  methanol) was derivatized with GirT (5 mg/mL in methanol containing 0.1% trifluoroacetic acid (TFA)) by heating (40 °C, 60 min), and the reaction was stopped with water (50  $\mu\text{L}$ ). Nonderivatized and derivatized steroids were analyzed by LC-MS/MS (QTrap 5500 triple quadrupole MS (Sciex, Warrington, UK) interfaced with an Acquity UPLC (Waters, Manchester, UK)). Separation was achieved using a Kinetix C18 column (Phenomenex, Macclesfield, UK; 150 cm, 3 mm, 2.6  $\mu\text{m}$ ; 35 °C). Initial mobile phase conditions were water with 0.1% formic acid/methanol (70:30), changing to 20:80 from 1 to 10 min, and

then sustained until 15.5 min. Selected ion monitoring detected nonderivatized and derivatized steroids, respectively, testosterone ( $m/z$  289.1, 402.3) and DHT ( $m/z$  291.1, 404.2) with electrospray (ESI) MS (source temperature, 30 °C; ion source gases GS1 and GS2 (50 and 70, respectively); CAD low; ion spray voltage, 5500 V; curtain gas, 40 psi; entrance potential, 10 V).

**Imaging Instrumentation.** MSI was performed first by 12T SolariX MALDI-FTICR-MS (Bruker Daltonics, MA, US) employing a Smartbeam 1 kHz laser, operated with SolariX control v1.5.0 (build 42.8), Hystar 3.4 (build 8), and FlexImaging v3.0 (build 42). Confirmatory on-tissue collision induced dissociation (CID) was carried out by liquid extraction surface analysis (LESA)-nanoESI-FTICR-MS (Triversa Nanomate, Advion, New York, USA). Secondly high spatial resolution imaging was performed using a MALDI q-TOF MS (MALDI Synapt G2 HDMS, Waters). Regions of interest (ROIs) were defined. Image files were generated in Mass Lynx (v4.1) and then viewed in HDI Imaging (v1.2).

**Tissue Sectioning and Mounting.** Tissue was embedded in gelatin (50% w/v). Top-down (horizontal) sections of testes (10  $\mu\text{m}$ ) were thaw mounted onto conductive indium tin-oxide (ITO)-coated glass slides (Bruker Daltonics, Bremen, GmbH) and stored in a vacuum desiccator (RT, 1 h) and then at –80 °C. Adjacent sections were stained using hematoxylin and eosin. After fixation in cold acetone, tissue sections were examined using an optical microscope (40X, Leica Microsystems Inc., Bannockburn, IL, USA) with CCD camera (Hitachi, 3969, Japan).

**Detection of Endogenous Steroids in Rodent Tissues without Derivatization.** Tissues were prepared and matrix applied ( $\alpha$ -cyano-4-hydroxycinnamic acid; CHCA) as below.

**Detection of Endogenous Steroids in Rodent Tissues Following OTCD.** From –80 °C, tissue sections were dried in a vacuum desiccator (20 min). Derivatization reagent (GirT, 5 mg/mL methanol/water (80:20) with 0.1% TFA containing *d*<sub>8</sub>-CORT (10  $\mu\text{g}/\text{mL}$ )) was applied by an artistic airbrush,<sup>14</sup> with a reagent density of 0.11 mg/cm<sup>2</sup>. The procedure for reagent and matrix application<sup>14</sup> was automated for higher resolution imaging. The reagent was applied (flow rate 90  $\mu\text{L}/\text{min}$ ) by an automated sprayer (HTX Technologies, Carrboro, North Carolina, US). Nebulization gas was nitrogen (10 psi). The nozzle spray (100 °C, positioned ~35 mm from the target) was deposited (linear velocity, 850 mm/min; offset spacing, 3 mm). Ten passes were performed leading to a matrix density of 0.21 mg/cm<sup>2</sup>, matched to manual matrix spraying.<sup>14</sup> On alternate passes, the spray pattern was offset by 1.8 mm. After derivatization, the slide was placed in a temperature/humidity controlled chamber (Memmert HPP 110, Schwabach, GmbH; 40 °C, 80% relative humidity) in a sealed slide box. The tissue was incubated (60 min, 40 °C) and then allowed to cool and dry in a vacuum desiccator (RT, 15 min) to remove the condensed water prior to matrix deposition.

**Matrix Application.** CHCA (10 mg/mL in acetonitrile (80%) + 0.2% v/v TFA) was applied by a pneumatic TLC sprayer (20 mL/slide; nitrogen flow, 7.5 L/min; distance 20 cm from target). Each manual pass took ~1 s and was repeated with 5–10 s between passes, until uniform coating was achieved. The tissue section was allowed to dry (RT) and stored in a desiccator. For higher resolution studies, the matrix was applied by an automated sprayer as above except that the nozzle was 90 °C and linear velocity was 1100 mm/min.

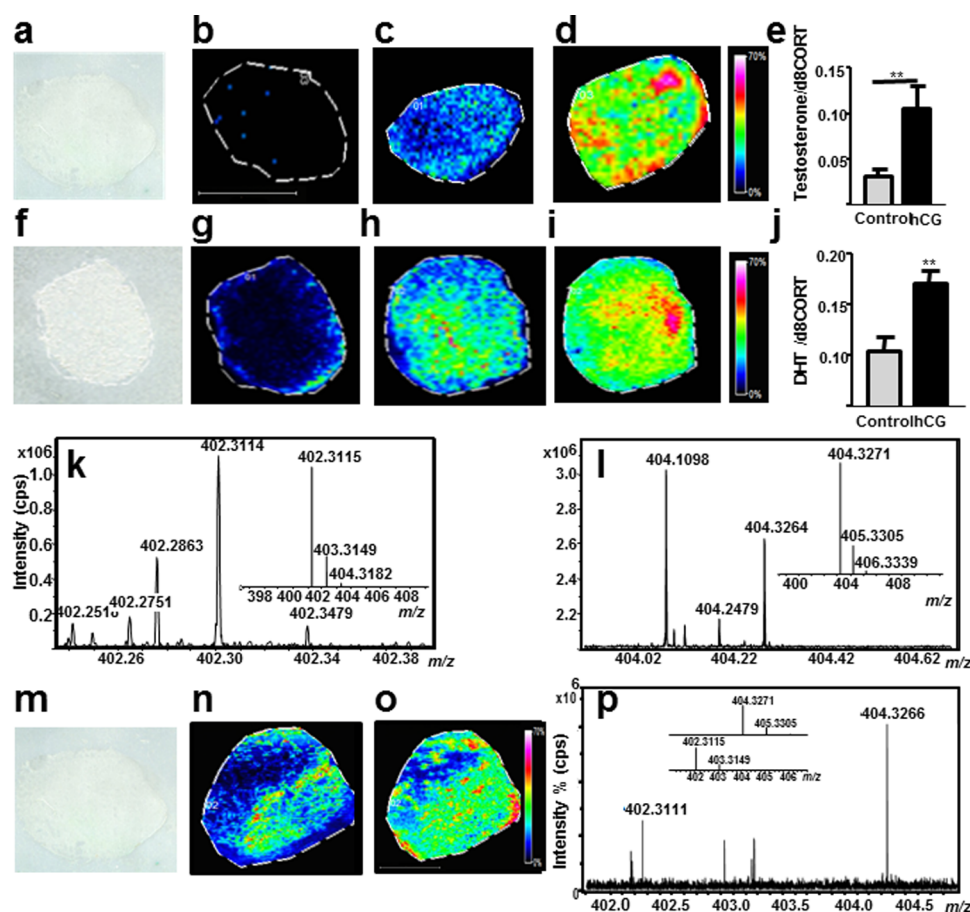


**Figure 1.** Molecular imaging by MALDI-FTICR-MSI of androgens analyzed intact and as Girard T derivatives in murine testes. Nonderivatized steroids could not be detected in testes even following stimulation with human chorionic gonadotrophin (hCG). However, upon derivatization, testosterone and  $\Delta^5$ -dihydrotestosterone (DHT) were detected. Optical images of a cryosection of murine testis (a, f) or rat prostate (m). Molecular image of (b) nonderivatized testosterone at  $m/z$  289.2098  $\pm$  0.005 Da in an hCG-stimulated mouse. Derivatized testosterone at  $m/z$  402.3114  $\pm$  0.0005 Da in testes from (c) control and (d) hCG stimulated mouse. (e) The relative abundance of testosterone (corrected for internal standard, corticosterone- $d_8$  ( $d_8$ -CORT)) was increased  $\sim$ 2.5-fold following hCG stimulation. Molecular image of (g) nonderivatized DHT at  $m/z$  291.2112  $\pm$  0.0005 Da in an hCG stimulated mouse. Derivatized DHT at  $m/z$  404.3264  $\pm$  0.0005 Da in testes from (h) control and (i) hCG stimulated mouse. (j) The relative abundance of DHT (corrected for internal standard) was increased  $\sim$ 1.8-fold following hCG stimulation. Derivatized testosterone (n) and DHT (o) in rat prostate. Representative FTICR-MS spectrum of (k) testosterone and (l) DHT hydrazone in mouse testes and (p) both steroidal derivatives in rat prostate showing excellent agreement (mass accuracy  $\pm$  5 ppm) with simulated theoretical isotopic distribution pattern (embedded). Data are mean  $\pm$  SEM;  $n$  = 3 mice per group; cps = counts per second; scale bar = 2 mm. Signal intensity is depicted by color on the scale shown. \*\* =  $p$  < 0.01 compared by Student  $t$ -test.

**MALDI-FTICR-MSI Analysis.** Optical images were scanned (Canon LiDE-20, Canon, UK). MSI analysis was performed using constant accumulation of selected ions (CASI) using a 80 Da isolation window centered at 435 Da yielding a 2 Mword time-domain transient. Laser spot diameter was 100  $\mu$ m, and raster spacing was 100–300  $\mu$ m. Laser shots were 800 and power optimized for consistent ion production. MSI data were subject to window normalization to  $m/z$  of 468.3064 (GirT- $d_8$ -CORT). Mass precision was typically  $\pm$ 0.0005 Da. Average abundances were assigned from the summed spectra within ROIs. Neutral testosterone and DHT were analyzed (without derivatization) in positive mode at  $m/z$  289.2098 and  $m/z$  291.2112. Ions of derivatives were monitored in positive mode:  $m/z$  402.3115 (GirT-testosterone) and 404.3271 (GirT-DHT). The CHCA matrix ions at positive  $m/z$  417.0483, along with GirT- $d_8$ -CORT, were monitored to assess uniformity of matrix application.

**Higher Spatial Resolution Analysis.** Using a MALDI q-TOF MS, the ROI was defined and the spatial resolution set (50  $\mu$ m). Positive ion data were acquired in sensitivity mode (target

enhancement at  $m/z$  402) with 350 laser shots/raster position using a 1 kHz laser. Optimization was achieved by tuning acquisition settings while collecting data from a control spot of analytes (0.5  $\mu$ L, 0.1 g/mL of standard at  $\sim$ 2  $\mu$ m manually spotted with an equal volume of derivatization solution/matrix). Ions formed by derivatives were monitored in positive mode:  $m/z$  402.31 (GirT-testosterone) and  $m/z$  404.33 (GirT-DHT). Mass filter windows were selected with a precision of  $\pm$ 0.04 Da. Data were normalized by total ion current.

**Liquid Extraction Surface Analysis (LESA)-ESI-FTICR-MS.** Steroids within tissue sections were derivatized<sup>14</sup> and analyzed immediately using LESA-nanoESI-FTICR-MS with the 12T SolariX ESI-MALDI source: solvent, methanol/water, 50:50 with 0.1% v/v of formic acid; pick-up volume, 1.5  $\mu$ L; dispense volume, 1.2  $\mu$ L at 0.2 mm from surface; droplet rest time (delay), 5 s; aspiration volume of 1.4  $\mu$ L at 0.0 mm from surface. Ions were detected between  $m/z$  250 and 1500, with an isolation window of 0.1 Da, yielding a 2 Mword time-domain transient.

Ions of GirT-hydrazones (as MALDI) were isolated (30 s) prior to selection of  $m/z$   $400.3 \pm 5$  for CID performed at 32 eV.

**Limits of Detection.** Limits of detection were assessed by spotting serial dilutions of steroid solutions (0.1–100 pg) onto slides and also control sections (murine brain) and assessed by MALDI-FTICR-MS. Data were compared using Student's *t*-test (Statistica version 8.0, StatSoft, Inc., Tulsa, OK, USA).

## RESULTS AND DISCUSSION

**Mass Spectral Characterization of Steroids.** The mass spectra of nonderivatized androgen standards contained protonated molecular ions (testosterone,  $m/z$  289.2098; DHT,  $m/z$  291.2112). Initial imaging attempts to detect nonderivatized androgens in mouse testes were unsuccessful, as signal-to-noise ratios (SNR)  $< 2$  (Figure 1b,g), even following hCG stimulation. This resembles glucocorticoids, which are also undetectable in their native state by ourselves<sup>14</sup> and others.<sup>16</sup> Accordingly, GirT derivatives were formed and reactions were monitored using ESI, which allowed concomitant assessment of native and derivatized forms. With ESI, the steroid signal intensities were boosted by  $\sim 20$ – $30\times$  by derivatization. However, reaction efficiencies differed with DHT, reacting  $\sim 5$  times more slowly than testosterone, due to its less reactive 3-ketone.

Reaction conditions were subsequently optimized on-tissue using testosterone. The MALDI MS spectra of the GirT-hydrazones yielded  $[M]^+$  ions, with masses at  $m/z$  402.3114 for testosterone (Figure 1k) and  $m/z$  404.3264 for DHT (Figure 1l), in close agreement with theoretical masses. As before, GirT derivatives yielded spectra dominated by the molecular ion and high resolution MS overcame the challenge of selecting specific analytes from high abundance ions in the low mass range emanating from matrix and tissue. Structural confirmation was performed within tissue by CID using LESA-ESI-FTICR-MS, allowing isolation experiments to be performed with greater sensitivity than could be achieved during MALDI imaging (CID mass spectra, Figure S-2). CID of GirT-testosterone generated fragment ions ( $m/z$  343 and 315) characteristic of loss of the quaternary amine tag  $[M-59]^+$  and carbon monoxide  $[M-87]^+$ , respectively, from the derivatized group. Similar fragmentation occurred with GirT-DHT. Proposed patterns (Proposed Fragmentation Patterns, Figure S-2) agreed with the fragmentations of GirT derivatives of glucocorticoids<sup>14</sup> and also those of GirP steroid hydrazones, which may form stable five membered rings.<sup>18</sup> Further androgens (androstenedione, DHEA) were also successfully derivatized with GirT (Mass spectrum, Figure S-3). Notably, GirT-DHEA gave the same precursor ion as testosterone and fragmented similarly under LESA conditions, unless high energy was applied.

OTCD and matrix application were adapted for automated spraying, allowing greater control of crystal size and topological homogeneity, aiming to improve spatial resolution and reduce the likelihood of hot spots. Previously, deposition of methanolic solutions was by either a manual TLC sprayer or airbrushes, where the distance from target and nozzle–nozzle reproducibility were difficult to control, varying between suppliers and even lots. Nonetheless, a good spray mist could be achieved, leading to a homogeneous layer of reagent, good analyte extraction, and desirable cocrystallization. However, reproducibility was highly analyst dependent and analyte diffusion was a concern through repeated wetting.

Sublimation (solvent-free) was piloted, leading to smaller crystal size but poor tissue-extraction, particularly with hydrophobic analytes. Shimma et al. report a successful dual approach

of sublimation and airbrushing to reduce crystal size.<sup>16</sup> Ultimately, automated deposition was used, improving reproducibility and crystal size homogeneity but requiring extensive optimization of spray parameters (nozzle temperature, nitrogen flow, solvent composition, solvent flow rate, surface tension) to achieve good analyte extraction. A balance between “not too wet”, promoting diffusion, and “not too dry”, impeding analyte extraction, was struck. Our experience is that, while reproducibility is improved by automated spraying, better sensitivity/extraction may still be observed using an airbrush. Furthermore, automatic sprayers require instrument-specific optimization.

**Relative Quantitation of Derivatized Steroids.** CASI was used to maximize signal intensity and limits of detection (LODs) of derivatized testosterone were  $\sim 0.1$  pg (off-tissue) and 1 pg (on-tissue; SNR 21). GirT derivatives of testosterone yielded ions of similar intensity to GirT- $d_8$ -CORT; similar ionization efficiency is anticipated,<sup>14</sup> for steroids with an activated A-ring ketone. However, the yield of GirT-DHT was lower due to reduced reactivity of the nonconjugated ketone moiety. Therefore, relative quantitation between testosterone and DHT requires normalization, readily achievable with stable-isotope labeled internal standards. <sup>13</sup>C labeling is preferred to deuterium due to the potential for loss of deuterium during derivatization or fragmentation.<sup>19</sup>

**Detection of Endogenous Steroids in Rodent Tissues.** GirT derivatives of androgens were successfully detected using two imaging MS platforms. Initially, studies were performed by MSI (with FTICR) at 150  $\mu\text{m}$  spatial resolution in murine testes, detecting steroids with mass accuracy of  $\pm 5$  ppm from their theoretical monoisotopic mass (Figure 1k,l). Androgens were detected in control testes (Figure 1c,h) with SNR of  $22 \pm 5$  and  $43.5 \pm 4$  for derivatized testosterone and DHT, respectively. Testosterone and DHT were in higher abundance following stimulation with hCG (Figure 1d,i) and SNR,  $265 \pm 11$  and  $387 \pm 13$ , respectively. The absolute signal intensity of testosterone and DHT relative to  $d_8$ -CORT was increased  $\sim 2.5$ - and  $\sim 1.8$ -fold by hCG (Figure 1e,j), respectively. Corresponding concentrations of testosterone in plasma rose from  $4.5 \pm 0.7$  to  $29.6 \pm 1.8$  nM following hCG, typical of the protocol.<sup>20</sup> Shimma et al. reported an increase of greater magnitude but over a shorter timecourse.<sup>16</sup>

The distributions of testosterone and DHT following hCG stimulation were assessed at higher spatial resolution (50  $\mu\text{m}$ ) using a MALDI-q-TOF instrument. In CASI mode on the SolariX (800 laser shots/pixel), a decline in sensitivity after 20 000 pixels was observed, possibly due to an accumulation of matrix/reagent ion clusters in the source; this was not observed by qTOF-MS. The steroid derivatives yielded the same molecular ions as with FTICR. The mass resolution was  $\sim 20$  000 (at  $m/z$  400) as opposed to 350 000, and the difference in mass accuracy of selected ions was  $< 5$  ppm versus their theoretical monoisotopic masses (Figure 2g). Potential interfering ions within the mass window were not evident in either the qTOF or the FTICR spectra from mouse testes. DHT was also detected but with a different spatial distribution. Testosterone was mainly localized within the seminiferous tubules (Figure 2a,c), while DHT was mainly observed in the interstitium/Leydig cells (Figure 2b,d). Although Shimma et al.<sup>16</sup> report Leydig cell localization of testosterone, their images display a clear signal in seminiferous tubules, in keeping with ours.

The method was subsequently applied to prostate tissue.  $5\alpha$ -Reductases are pharmacological targets within prostate, since suppression of DHT production attenuates growth of both

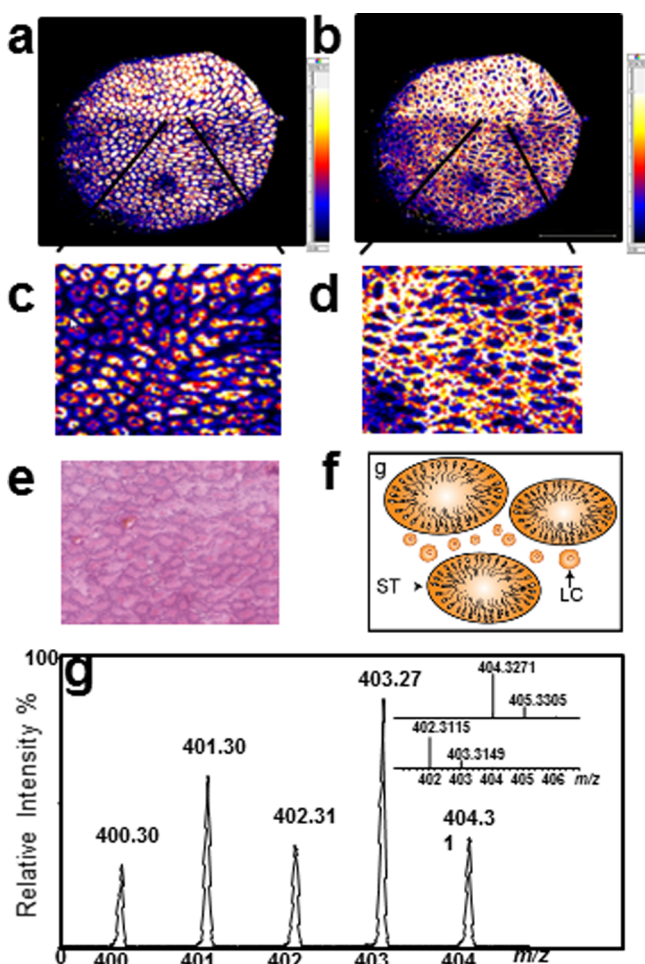


**Figure 2.** Molecular imaging of testosterone and  $5\alpha$ -dihydrotestosterone (DHT) Girard T derivatives in rodent testes at  $50\ \mu\text{m}$  spatial resolution by MALDI-qTOF-MSI. Images of testes from mice stimulated with human chorionic gonadotrophin. (a) Derivatized testosterone at  $m/z\ 402.31 \pm 0.02\ \text{Da}$ . (b) Derivatized DHT at  $m/z\ 404.33 \pm 0.02\ \text{Da}$ . (c)  $15\times$  zoom image of (a). (d)  $15\times$  zoom image of (b). (e)  $15\times$  zoom of hematoxylin and eosin stained section of mouse testis. (f) Cartoon of testicular architecture (ST = seminiferous tubule, LC = Leydig cells). (g). Mass spectra of steroid derivatives detected in testes detected by MALDI-qTOF-MSI. Signal intensity is depicted by color on the scale shown. Scale bar (2 mm).

hyperplastic and cancerous tissue. Both testosterone and DHT could be detected  $\text{SNR} > 10$  (Figure 1n–p), suggesting that the MSI approach may open doors to pathological investigations of cell-specific androgen synthesis in prostate disease.

## CONCLUSIONS

Derivatization permits detection of poorly ionizable endogenous androgens in target tissues by MSI. The use of Gir T reagent affords low limits of detection, similar to glucocorticoids.<sup>14</sup> OTCD proceeded rapidly for testosterone but was less efficient for DHT. However, both steroids were detected in tissue. For relative quantitation, commercial stable-isotope labeled androgens would allow data collection within a narrower mass window of  $\pm 5$  or  $10\ \text{Da}$  (as opposed to  $80\ \text{Da}$  using  $d_8$ -CORT), potentially improving sensitivity.

OTCD coupled with MALDI-FTICR-MSI successfully detected androgens in murine testes. A proof-of-principle experiment, representative of healthy biological variations in

tissue steroid levels, was performed using hCG to maximally stimulate androgen synthesis, achieving an increase in plasma testosterone which was also reflected in testicular steroids. Initial studies were performed at  $150\ \mu\text{m}$  resolution, detecting androgens in testes but without meaningful molecular histology. The seminiferous tubules of mice are  $\sim 300\ \mu\text{m}$  in diameter, and hence, smaller laser bores were required to reveal the characteristic tissue structure, although this may be less challenging in larger species. Higher resolution imaging ( $50\ \mu\text{m}$ ) localized testosterone and DHT to different compartments of the adult mouse testis.

The need for higher resolution imaging brings with it concerns over analyte diffusion, matrix crystal size, and tissue integrity. Manual application of matrix and reagent, while effective, was subject to variability between operators. The automated application allows better tissue–tissue reproducibility and improved homogeneity of matrix coverage compared with TLC sprayers or airbrushes. Future optimization of OTCD and matrix application by sublimation may allow even higher spatial resolution, possibly  $5\ \mu\text{m}$  approaching cellular resolution, now obtainable with new MALDI systems.

MSI with OTCD is a powerful tool to study the regional variation in abundance of androgens in tissues, and here, we broaden the scope of the technique to reproductive biology. In translating to nonrodent tissues, the presence of isobaric steroids and highly abundant DHEA, as well as epi-testosterone, must be considered. Although underivatized DHEA fragments differently from testosterone under tandem MS conditions, the predominant fragment of the derivatives within FTICR or the qTOF is the derivatizing group, militating against their discrimination in the absence of chromatography. Other approaches such as MSn as reported with the IMScope<sup>16</sup> or ion mobility may permit isomeric separation, as required by translational research.

## ASSOCIATED CONTENT

### Supporting Information

The Supporting Information is available free of charge on the ACS Publications website at DOI: 10.1021/acs.analchem.6b02242.

Figure S-1: Steroid nomenclature and derivatization reaction schemes to form Girard T derivatives of common endogenous androgens. Figure S-2: Mass spectra and proposed fragmentation patterns of the Girard T derivative of testosterone and dihydrotestosterone collected following liquid extraction surface analysis with nanoESI-FTICR collision induced dissociation. Figure S-3: MALDI-FTICR-MS spectra and collision-induced fragmentation of a mixture of androstenedione and dehydroepiandrosterone derivatized with Girard T reagent (PDF)

## AUTHOR INFORMATION

### Corresponding Author

\*Tel: +44 (0) 131 242 6763. Fax: +44(0) 131 242 6779. E-mail: ruth.andrew@ed.ac.uk.

### Present Address

<sup>V</sup>D.F.C.: Biomedical Sciences Research Institute, School of Biomedical Sciences, University of Ulster, Coleraine campus, Cromore Road, Coleraine, Co. Londonderry, BT52 1SA, UK.

### Author Contributions

<sup>¶</sup>D.F.C. and D.E.W.L. are joint first authors.

## Notes

The authors declare no competing financial interest.

## ACKNOWLEDGMENTS

We acknowledge funding from the Medical Research Council (MC\_PC\_12014), the British Heart Foundation (RG-05-008), and its Centre for Research Excellence (BHF RE/08/001). B.R.W. is a Wellcome Trust Senior Investigator.

## REFERENCES

- (1) O'Shaughnessy, P. J.; Baker, P. J.; Heikkila, M.; Vainio, S.; McMahon, A. P. *Endocrinology* **2000**, *141*, 2631–2637.
- (2) Shima, Y.; Miyabayashi, K.; Haraguchi, S.; Arakawa, T.; Otake, H.; Baba, T.; Matsuzaki, S.; Shishido, Y.; Akiyama, H.; Tachibana, T.; Tsutsui, K.; Morohashi, K. *Mol. Endocrinol.* **2013**, *27*, 63–73.
- (3) Mahendroo, M. S.; Cala, K. M.; Hess, D. L.; Russell, D. W. *Endocrinology* **2001**, *142*, 4652–4662.
- (4) Imperato-McGinley, J. *European Urology* **1994**, *25*, 20–23.
- (5) Bartsch, G.; Rittmaster, R. S.; Klocker, H. *World J. Urol.* **2002**, *19*, 413–425.
- (6) Wen, Q.; Cheng, C. Y.; Liu, Y. X. *Semin. Cell Dev. Biol.* **2016**, DOI: 10.1016/j.semcdb.2016.03.003.
- (7) Labrie, F. *Semin. Reprod. Med.* **2004**, *22*, 299–309.
- (8) Longcope, C. *Menopause* **2003**, *10*, 274–276.
- (9) Smith, L. B.; Walker, W. H. *Semin. Cell Dev. Biol.* **2014**, *30*, 2–13.
- (10) Carson, C., III; Rittmaster, R. *Urology* **2003**, *61*, 2–7.
- (11) Schmitz-Drager, B. J.; Fischer, C.; Bismarck, E.; Dorsam, H. J.; Lummen, G. *Urologe A* **2007**, *46*, 1364–1370.
- (12) Miyoshi, Y.; Uemura, H.; Umamoto, S.; Sakamaki, K.; Morita, S.; Suzuki, K.; Shibata, Y.; Masumori, N.; Ichikawa, T.; Mizokami, A.; Sugimura, Y.; Nonomura, N.; Sakai, H.; Honma, S.; Harada, M.; Kubota, Y. *BMC Cancer* **2014**, *14*, 717.
- (13) Chughtai, K.; Heeren, R. M. A. *Chem. Rev.* **2010**, *110*, 3237–3277.
- (14) Cobice, D. F.; MacKay, C. L.; Goodwin, R.; McBride, A.; Langridge-Smith, P.; Webster, S. P.; Walker, B. R.; Andrew, R. *Anal. Chem.* **2013**, *85*, 11576–11584.
- (15) Shackleton, C. H.; Chuang, H.; Kim, J.; de la Torre, X.; Segura, J. *Steroids* **1997**, *62*, 523–529.
- (16) Shimma, S.; Kumada, H.-O.; Taniguchi, H.; Konno, A.; Yao, I.; Furuta, K.; Matsuda, T.; Ito, S. *Anal. Bioanal. Chem.* **2016**, DOI: 10.1007/S00216-016-9594-9.
- (17) Upreti, R.; Naredo, G.; Faqehi, A. M. M.; Hughes, K. A.; Stewart, L. H.; Walker, B. R.; Homer, N. Z. M.; Andrew, R. *Talanta* **2015**, *131*, 728–735.
- (18) Griffiths, W. J.; Wang, Y. *Biochim. Biophys. Acta, Mol. Cell Biol. Lipids* **2011**, *1811*, 784–799.
- (19) Faqehi, A. M. M.; Cobice, D. F.; Naredo, G.; Mak, T. C. S.; Upreti, R.; Gibb, F. W.; Beckett, G. J.; Walker, B. R.; Homer, N. Z. M.; Andrew, R. *Talanta* **2016**, *151*, 148–156.
- (20) Rebourcet, D.; Wu, J.; Cruickshanks, L.; Smith, S. E.; Milne, L.; Fernando, A.; Wallace, R. J.; Gray, C. D.; Hadoke, P. W. F.; Mitchell, R. T.; O'Shaughnessy, P. J.; Smith, L. B. *Endocrinology* **2016**, *157*, 2479–2488.